ABSTRACT

Title of Thesis:	DIEL GREENHOUSE GAS EMISSIONS DEMONSTRATE A STRONG RESPONSE TO VEGETATION PATCH TYPES IN A FRESHWATER WETLAND
	Aileen Taylor, Master of Science in Environmental Science and Technology, 2022
Thesis directed by:	Dr. Margaret Palmer, Department of Entomology

Wetland methane (CH_4) fluxes are highly variable over spatial and temporal scales due to variations in the functional controls of CH_4 production, oxidation, and transport. While some aspects of temporal variability in CH_4 fluxes are well documented (like seasonal patterns), diurnal variability is still poorly constrained. Existing studies report conflicting evidence of diurnal patterns so we cannot make broad generalizations about diurnal patterns of CH_4 flux. This is further confounded by the within-wetland spatial heterogeneity that characterizes many wetland systems: variations in topography, soil chemistry, hydrologic regime, and vegetation type can result in characteristically different "patches" that could likely influence existing diurnal patterns. Limited availability of nighttime data due to current methodological constraints also limits our ability to make broad generalizations about CH_4 flux patterns. I investigated the diurnal patterns of CH_4 fluxes in a seasonal-mineral soil wetland on the Delmarva Peninsula (Maryland, USA) across three functionally unique patches: two with vegetation (emergent and submerged aquatic vegetation), and one without (open water) during the summer of 2021. To explore the potential relationship

between physicochemical variables and flux patterns, we also measured a series of physicochemical variables including temperature (air and water), relative humidity, PAR, DO, etc. To my knowledge, this is the first study to compare diel variability across these three patch types. We found that diel patterns in wetland systems are strongly linked to the dominant vegetation cover of a patch, but whether these differences in patterns are a direct result of vegetation impact on production, oxidation and/or transport of CH_4 or on patch-specific conditions that covary with patch type will require extended study. Ultimately, this study contributes to the growing understanding of how CH_4 flux vary spatially over diel cycles.

DIEL GREENHOUSE GAS EMISSIONS DEMONSTRATE A STRONG RESPONSE TO VEGETATION PATCH TYPES IN A FRESHWATER WETLAND

by

Aileen K. Taylor

Thesis submitted to the Faculty of the Graduate School of the
University of Maryland, College Park, in partial fulfillment
of the requirements for the degree of
Masters of Science
2022

Advisory Committee:
Dr. Margaret Palmer, Chair
Dr. Andrew Baldwin
Dr. Stephanie Yarwood
Dr. Greg McCarty

Dedication

This thesis is dedicated to my family: to my parents, Maureen and John, who supported me every step of the way and have listened to me ramble about my work, to my siblings, Johnny, Mary, Patrick, Julia, and Cathy, and to Carly, Anna, Clare, little Johnny. Without their loved and support (and their endearing heckling: “If you write enough paragraphs, you’ll become a doctor!”), none of this would’ve been possible.

This is also dedicated to my dear friends who supported me: to Kat and Mariah, who stayed up with me on long skype calls as I worked, and to Christine, Margaret and Gretchen, who put up with field equipment slowly taking over our house and were the best roommates I could’ve asked for here in Maryland. This would not have been possible without all of you. Thank you.

Acknowledgements

None of this would have been possible without the team of people who helped and guided me throughout these past few years.

I would like to thank my advisor, Margaret, for her guidance and support both in developing, conducting, and writing this project. I would also like to thank my committee members for their contributions and guidance: Dr. Baldwin, Dr. Yarwood, and Dr. McCarty. I would also like to thank the National Socio-Environmental Synthesis Center.

I would also like to thank everyone in the Palmer lab, without whom none of this would've been possible. I am especially thankful to Alec Armstrong who accompanied during my 24-hour sampling (none of this would've happened without his help). Special thanks as well goes to Graham Stewart and Sean Sharp, who offered valuable help and insight in all stages of this process. In addition, I'd like to thank James Maze, Michael Williams, Christine Maietta, and Kelly Hondula for their help and support throughout these last few years.

Table of Contents

List of Tables

List of Figures

List of Abbreviations

EmVeg	Emergent vegetation patch
SubVeg	Submerged aquatic vegetation patch
NoVeg	No vegetation patch
DO	Dissolved oxygen
PAR	Photosynthetically active radiation

1. Introduction

Wetland ecosystems are vital sources of carbon sequestration and are on average the most carbon dense terrestrial systems (Yang *et al.* 2017), storing 20% of global organic ecosystem carbon (Temmink *et al.* 2022). However, because of anaerobic conditions in saturated soils (Yang *et al.* 2017), wetlands are also the largest natural source of atmospheric methane (CH_4), contributing roughly 80-280 Tg CH_4 yr^{-1} (Bridgham *et al.* 2013). CH_4 has a global warming potential 25x greater than carbon dioxide (CO_2) over a 100 yr. period (Bridgham *et al.* 2013; Neubauer and Megonigal 2015; Bansal *et al.* 2018) and thus it is important to accurately measure and model current wetland CH_4 fluxes. Currently, there is high uncertainty in emission estimates, in part due to high spatiotemporal variability within and among wetlands (Bansal *et al.* 2018).

Temporally, research has documented pronounced seasonal patterns in wetland CH_4 fluxes (Wilson *et al.* 1989; Duan *et al.* 2005; Chen *et al.* 2008; Morin *et al.* 2014; Poindexter *et al.* 2016), with higher fluxes in growing seasons (Morin *et al.* 2014; Poindexter *et al.* 2016). Fluxes are also known to vary annually, largely due to variation in weather patterns (Duan *et al.* 2005; Chen *et al.* 2008). On shorter time scales, there is some evidence that wetland CH_4 emissions vary diurnally (Mikkela *et al.* 1995; Godwin *et al.* 2013; Sun *et al.* 2013; Yu *et al.* 2013; Morin *et al.* 2014; Yang *et al.* 2017; Bansal *et al.* 2018); however, not all studies have found this (Henneberger *et al.* 2017; Milberg *et al.* 2017). Spatially, research has shown that fluxes can vary considerably even within the same climatic and soil regions (Neubauer and Megonigal

2022). Even within a wetland, variation in topography, soil chemistry, hydrological regime, and vegetation type results in different "patches" (Herbs *et al.* 2011) that can create dynamic spatial patterns in CH_4 fluxes (Baldocchi *et al.* 2012; Matthes *et al.* 2014) due to differences in CH_4 production, oxidation, and transport. Many factors that influence these three also vary diurnally (e.g., sunlight, temperature, etc.).

This within-wetland spatial heterogeneity or "patchiness" likely influences the potential for diel patterns in CH_4 emissions, especially if there is variable plant composition across patches (Villa *et al.* 2021). Fluxes from patches dominated by emergent vegetation often peak during the day (Whiting and Chanton 1996; Jeffrey *et al.* 2019) while fluxes from non-vegetated areas may peak during the night (Godwin *et al.* 2013; Poindexter *et al.* 2016). This may be due to differences in the dominant transport mechanism of CH_4 flux in each patch. In emergent vegetated patches, plant-mediated transport is likely the dominant contributor to CH_4 flux (Poindexter *et al.* 2016; Bansal *et al.* 2020) so changes in plant activity (and associated opening/closing of stomata) driven by changing light levels will impact the magnitude/rate of CH_4 transport (Whiting and Chanton 1996; Jeffrey *et al.* 2019). In non-vegetated patches, hydrodynamic transport (i.e., molecular diffusion and wind driven or thermal-convective stirring of the water column) is likely the dominant contributor (Morin *et al.* 2014; Sieczko *et al.* 2020).

Wetland plants not only determine the dominant transport mechanism but themselves influence physicochemical drivers that impact CH_4 production and CH_4 oxidation. Depending on the plant species, increased plant activity has the potential to create either a more reducing environment by supplementing methanogens with

additional carbon substrates via root exudates or create a more oxidizing environment by increasing O_2 availability and potentially promoting CH_4 oxidation (Bhullar *et al.* 2013; Jeffrey *et al.* 2019; Noyce and Megonigal 2021). Submerged aquatic vegetation can also stimulate CH_4 oxidation in the water column, further reducing potential CH_4 flux (Masamba *et al.* 2015).

How all these factors interact to influence the presence of, or patterns in, CH_4 flux over day/night cycles is currently unknown. Sparse nighttime data limits our ability to make broad generalization about potential diel variability. The paucity of nighttime data is primarily due to limitation in the current methods for measuring fluxes, i.e., eddy covariance flux towers and chamber-based studies (Bansal *et al.* 2018). Eddy covariance methods allow for continuous measurements over large areas (Bridgham *et al.* 2013) but they also rely on turbulent air mixing which can be lacking at night. If the windshear drops below a certain threshold, the data are no longer reliable and must be discarded (Poindexter *et al.* 2017). Chamber-based studies often lack nighttime data due to the logistics of sampling in the dark, and thus rely on a single daytime flux measurement to estimate 24-hour fluxes (Pennock *et al.* 2010; Bansal *et al.* 2018) which may result in biased estimates.

In sum, more studies are needed to quantify potential diel patterns and nighttime CH_4 fluxes across a variety of systems. This would help improve global estimates of CH_4 fluxes and could potentially help elucidate the drivers of specific CH_4 flux patterns. This study in a seasonal-mineral soil wetland on the Delmarva Peninsula (Maryland, USA) sought to: 1) determine if there is diel variation in CH_4 fluxes and if CH_4 fluxes differ amongst patch types; 2) characterize patch-specific physicochemical

conditions; and, 3) explore potential relationships between CH_4 flux rates and physicochemical conditions. Based on previous studies, I expected to see fluxes in the emergent vegetation patch peaking during the day due to changing light levels influencing plant activity (Whiting and Chanton 1996; Jeffrey *et al.* 2019) I expected fluxes from the submerged aquatic to peak at night due to decreased plant activity and lower dissolved oxygen concentrations in the water column (Zhang *et al.* 2018). I also expected no vegetation patches to peak at night due to thermal stratification in the water column during the day (Godwin *et al.* 2013; Poindexter *et al.* 2016).

2. Methods

2.1 Study Site

The study site is in the Tuckahoe Creek, watershed a Coastal Plan subbasin on the Choptank watershed on the Delmarva Peninsula, USA. The climate is humid subtropic with 30-year average summer temperatures of 24°C, and 2.5°C in winter. Average annual precipitation is 110 cm (1985-2010 at Goldsboro, MD; PRISM climate mapping system); rainfall in 2021 was 112 cm.

The peninsula has ~17,000 freshwater depressional mineral wetlands, many of which are considered geographically isolated (Fenstermacher *et al.* 2014). These seasonal wetlands are classified as discharge areas from late fall to early spring and groundwater recharge basins during the summer when evapotranspiration (ET) is high (Phillips and Shedlock 1993). Because of widespread agricultural land use in the region, they are subject to a range of anthropogenic influence and disturbance (Fisher *et al.* 2006).

This study focused on a large wetland (~1.33 ha, 39°03’27”N, 75°45’12”W) (figure 1) that harbors diverse patches representative of wetlands in the broader region. Most of the wetlands have been drained for agriculture at some point (Fenstermacher *et al.* 2014). The study wetland was drained in the 1980s, converted to pastureland, then restored in 2003 by plugging ditches and removing woody vegetation. The mineral soils are Lenni loam (USDA-NRCS Soil Series) and major patch types based on their vegetation include: grass mats (*Panicum hemitomon*), sedge tussocks (*Carex striata*), low-growing emergent (*Persicari hydropiperaides*), aquatic vegetation

(*Juncus repens* and others), and open water (no vegetation). Like other wetlands in the region, the site is surrounded by forest dominated by *Nyssa sylvatica* (blackgum), *Liuidambar styraciflua* (sweetgum), and *Acer rubrum* (red maple) (Yepsen *et al.* 2014).

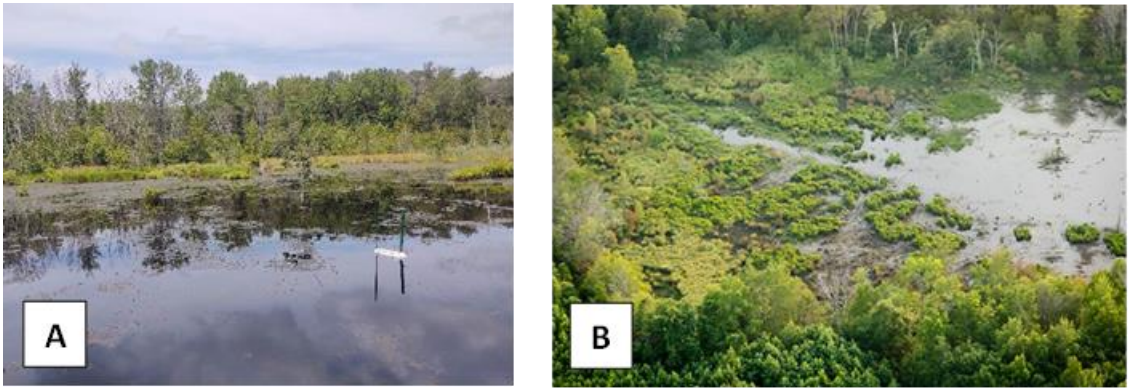

Figure 1. *(A) Ground photo of the study wetland (Credit: Sean Sharp). (B) Aerial photo of the study wetland (Credit: EPA Chesapeake Bay Program).*

2.2 Sampling Design

Three sampling campaigns were completed over the summer of 2021 (June 20th – 25th, July 26th – 30th, and September 12th – 17th). Within each campaign, gas fluxes were measured 6 times dispersed over two, 24-hour periods during the June campaign, and one 24-hour period during the July and September campaigns. Approximate sampling times were 9pm, 1am, 5am, 9am, 1pm, and 5pm. Measurements were made in each of 3 patch types that represent the dominant vegetation cover types: an emergent vegetation patch dominated by *Carex striata* (hereafter, EmVeg), a submerged aquatic vegetation patch dominated by *Juncus repens* (hereafter, SubVeg), and an open water patch with no standing vegetation (hereafter, NoVeg). Boardwalks were installed and spanned sampling patches to minimize soil and water disturbance during sampling.

2.3 Greenhouse gas emissions measurements

Gas fluxes were measured using floating chambers (n = 3 per patch type) in the SubVeg and NoVeg patches. The floating chambers (figures 2A, B, 40 x 40 x 40 cm) were designed (supplemental methods) based on the chambers used by Jeffrey *et al.* (2019), Rochette and Erisken-Hamel (2008), and Bastviken *et al.* (2020). Static chambers (figure 2C, 69.5 x 49.5 x 49.5 cm) designed based on Yu *et al.* (2013) were used in the EmVeg patch. The collars for the static chambers were installed a month prior to the start of sampling to allow impacted soils to recover after the initial disturbance of installation.

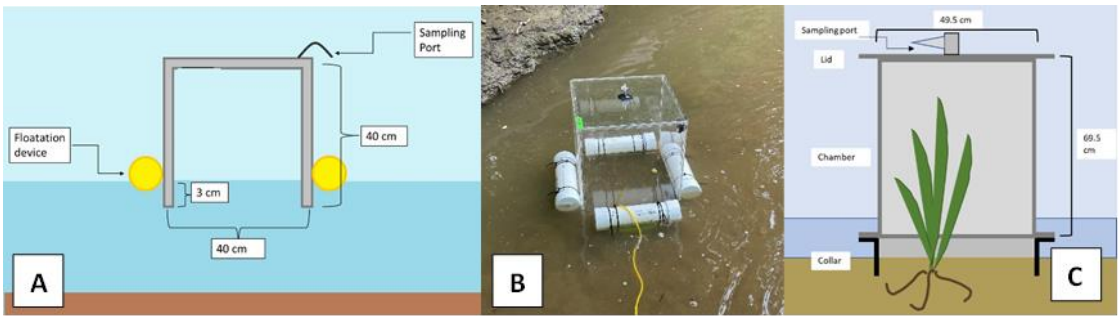

Figure 2*. (A) Floating chamber design. (B) Deployed floating chamber taken by Aileen Taylor. (C) Deployed static chamber design.*

2.4 Physicochemical measurements

At least a week prior to each sampling campaign, an array of sensors was deployed in each of the patch types to measure pH, temperature, and dissolved oxygen (DO); concentrations were measured at 5-minute intervals for ~3 weeks. Sensors were removed for data download and cleaning prior to relaunch before the next sampling campaign. Water column temperature (°C) was measured by a vertical series of

thermistor pendants (HOBO MX2202) at approximately every 5 cm. Water column pH and dissolved O_2 were measured just below the surface of the water column and at the sediment water interface using pH sensors (HOBO MX2501) and dissolved O_2 sensors (HOBO U26-001) respectively. Dissolved O_2 was not measured in the EmVeg patch due to equipment malfunction. Air pressure, air temperature, relative humidity (RH), and photosynthetically active radiation (PAR) measurements were taken via a flux tower located on site. Water depth was measured via wells installed in each patch.

2.5 Data analysis

Gas fluxes are reported as mean and standard error of three replicate samples for each time point. Data were categorized based on campaign, day of sampling, patch types, chamber, and time of day. Data were further split into "day" and "night" samples based on sampling time (day = 9am, 1pm, 5pm; night = 9pm, 1am, 5am) to differentiate between pre vs. post sundown. A series of repeated measures ANOVAs with nested subgroups (patches) were used to compare the rates of flux among the six different sampling times for each patch type. Repeated measures was used to account for potential autocorrelation between the same chamber. A least significant difference test was used to compare the means.

Physicochemical measurements resulted in time series for each 3-week period. Data are reported as mean and confidence interval for a 24-hour period at 5-minute intervals. To showcase potential stratification in the water column, the difference between the top and bottom of the water column over a 24-hour period is reported for each patch type (reported as `Temperature Difference`). The water column was

considered stratified if the temperature difference was greater than 1°C (after Woolway *et al.* 2014).

A Shapiro-Wilk Test was used to test for normality in the physicochemical datasets. As a preliminary analysis, a series of Kendall's correlations were run to determine if correlations between the physiochemical measurements and flux measurements were significantly different from 0. For the regression analyses described below, variance inflation factors (VIFs) were used to check for multicollinearity among variables: variables with values larger than 5 were removed from models. The relative importance of each variable was determined using partial R^2 values (a measure of the average contribution of each metric to the total variance accounting for all predictors). The finalized models were elected based on AIC_C scores. These regressions analyses were meant to be exploratory rather than inferential. The goal was to explore potential relationships between physicochemical variables and observed CH_4 fluxes to inform future work, not to create models to predict CH_4 fluxes. All analyses were done using R studio (v1.31073) (R Core Team 2022). Predictive models would require much larger data sets given the high variability that characterize gas fluxes as well as many of the physicochemical parameters (Bansal *et al.* 2018).

To explore the relationship between potential physicochemical drivers and observed CH_4 flux patterns, a series of multiple linear models were created using a combination of forward and backward stepwise progression. CH_4 flux data was natural log transformed with a nominal value prior to modeling. The first series (hereafter, "general patterns" model) was to explore potential relationships between flux magnitude, patch type, and physiochemical variables; all nine physicochemical

variables were included (biomass, water depth, air pressure, pH, humidity, PAR, water and air temperature, dissolved O_2). For modeling purposes, each patch was given a numeric indicator (EmVeg = 1, SubVeg = 2, and NoVeg = 3). This model identified patch type as a dominant variable, so subsequent analyses focused more specifically on diel variability were run separately for each patch type.

The second modeling series (hereafter, "patch specific diel patterns") was to explore potential relationships between CH_4 fluxes from each patch type and physicochemical variables that exhibited diel patterns (i.e., humidity, PAR, air and water temperature, and dissolved O_2).

3. Results

3.1 Objective 1: Variability in emissions

Within and across patch types, methane fluxes were highly variable over time. Emissions were positive throughout all sampling times for the emergent (figure 3) and submerged (figure 4) vegetation patches, while the no vegetation patch had negative fluxes at some of the sampling times (figure 5). The range in daily mean fluxes was greatest for the submerged vegetation patch type (5.07 – 90.62 mg CH_4 -C-m-2h-1), followed by the emergent patch (13.6 – 21.87 mg CH_4 -C-m-2h-1), and the no vegetation patch (0.05 – 3.93 mg CH_4 -C-m-2h-1) (figures 4 – 6). Consistently, the NoVeg patch had significantly lower average median fluxes than the other patches; however, these were not statistically different in July. Median fluxes in the EmVeg and SubVeg patches were similar except in September, when the EmVeg fluxes were significantly larger than fluxes from either of the other patch types (table S1).

Carbon dioxide fluxes were low or negative during the day but large at night for both the EmVeg and SubVeg patches. Both patches had repeated diel patterns such that they generally acted as CO_2 sinks during sunlight hours and CO_2 sources during dark hours but especially around 5am. NoVeg CO_2 fluxes were variable but did not display a repeated pattern (figures S1-3).

Diel patterns in methane were not consistent across patch types even though there was variation in emissions across sampling times. Instead, each patch type varied in terms of when peak and lowest emissions occurred. The EmVeg patch showed some evidence of significant diel variation during the June 23rd – 24th (F = = 3.39, df = 5,12,

p < 0.05), and September 12th -13th (F = 22.51, df = 5,12, p <0.001) campaigns; however, these differed between the two sampling periods and there were no significant differences between mean daytime (9am-5pm) and nighttime (9pm-5am) fluxes (figure 3).

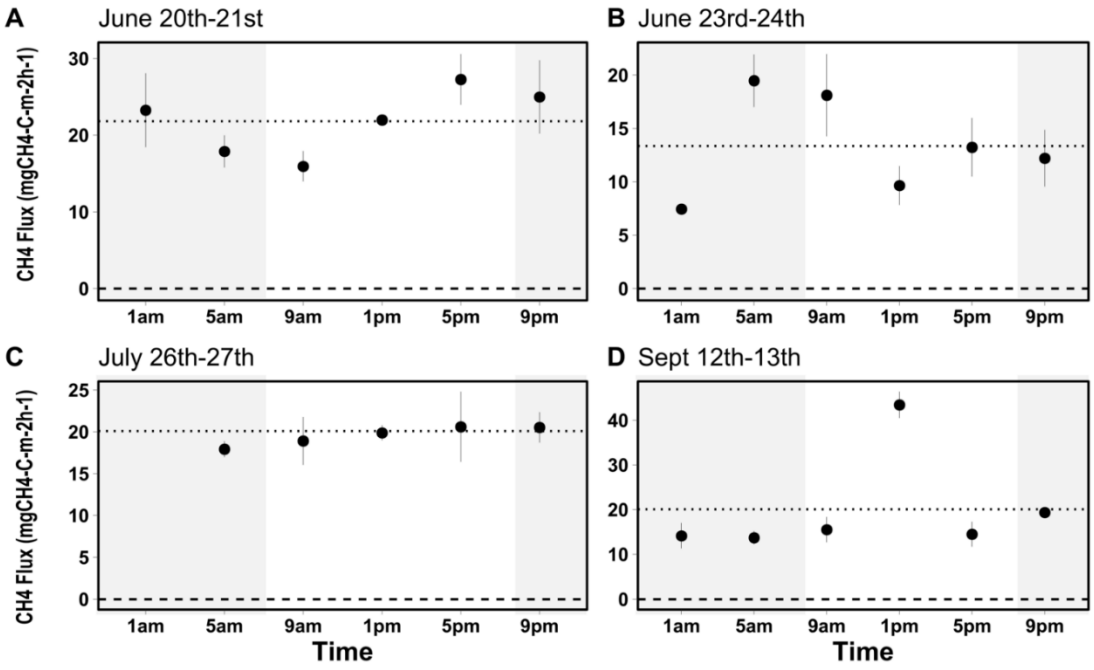

Figure 3. *Diel methane (CH_4) flux in the emergent vegetation patch (EmVeg) in a restored wetland in the Delmarva Peninsula, MD. Points are mean ± SE (n = 3) for six times during 4 sampling days over the summer of 2021. Different uppercase letters indicate significant differences among the sampling times (p < 0.05). Dotted line represents mean flux for that sampling period. Dashed line marks 0. Shaded region represents nighttime sampling. Axes are not standardized to showcase individual patterns exhibited during each sampling day.*

In contrast, fluxes from the submerged veg patches peaked at 1pm for three out of four sampling days, and these fluxes were much larger than the calculated average daily flux (figure 4). On July 28th, there was a large peak at 5am (mean = 201.8 ± 144.2

mgCH_4 -C-m-2h-1), which followed a brief rainstorm. Daytime fluxes (9am-5pm) were usually larger than nighttime fluxes (9pm-5am).

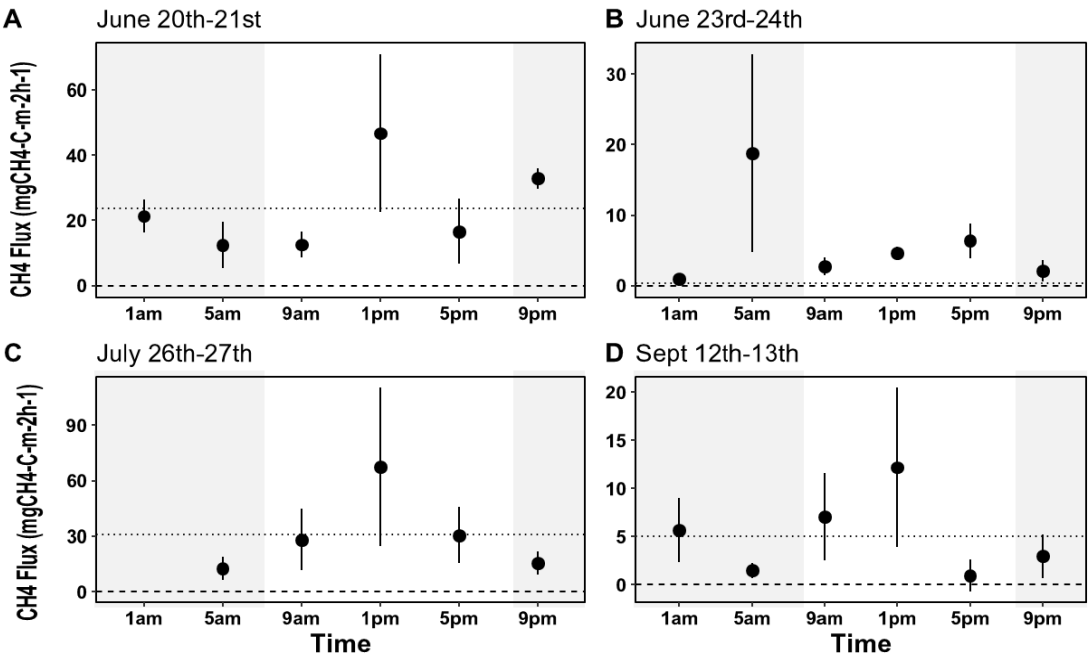

Figure 4. *Diel methane (CH_4) flux in the submerged aquatic vegetation patch (SubVeg) in a restored wetland in the Delmarva Peninsula, MD. Points are mean ± SE (n = 3) for six times during 4 sampling days over the summer of 2021. Different uppercase letters indicate significant differences among the sampling times (p < 0.05). Dotted line represents mean flux for that sampling period. Dashed line marks 0. Shaded region represents nighttime sampling. Axes are not standardized to showcase individual patterns exhibited during each sampling day.*

Fluxes from the NoVeg patch were extremely low excluding the July sampling: mean fluxes in July were significantly higher (means = 3.52, 4.02 mg mgCH_4 -C-m-2h-1) than the mean fluxes from both June and September ($F = 4.28$, df = 4, 66, $p < 0.01$) (table 1). Fluxes in this patch peaked at 5am and reached their lowest point at 1pm three out of four sampling days. This was the only patch type that consistently

displayed negative fluxes (mostly during the day) (figure 5). Daytime fluxes (9am-5pm) were usually lower than nighttime fluxes (9pm-5am).

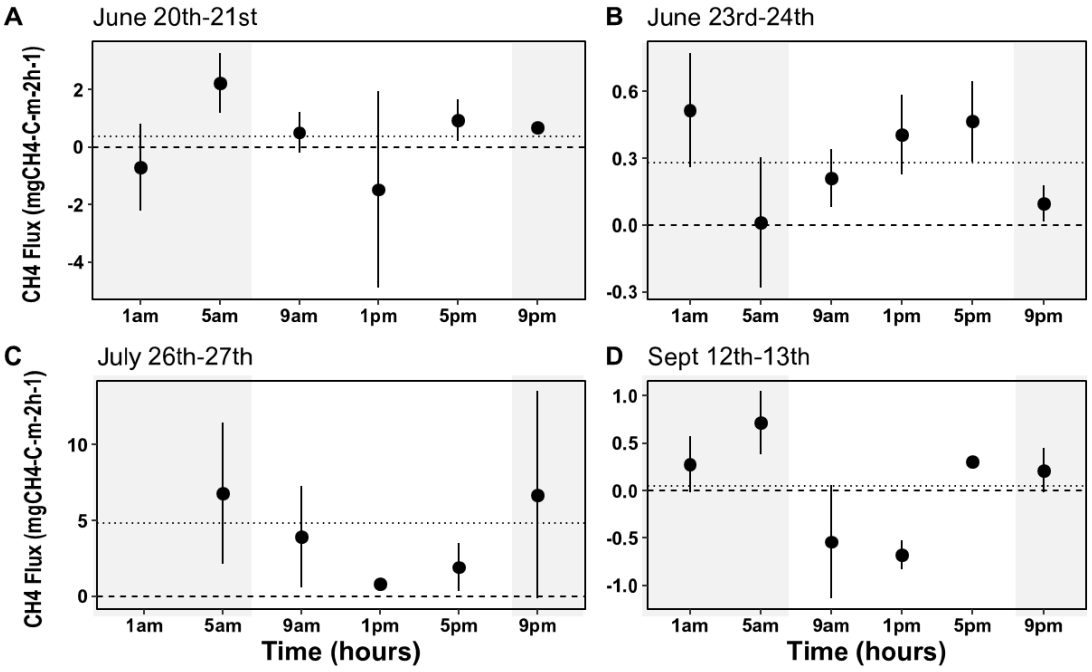

Figure 5. *Diel methane (CH_4) flux in the no vegetation patch (NoVeg) in a restored wetland in the Delmarva Peninsula, MD. Points are mean ± SE (n = 3) for six times during 4 sampling days over the summer of 2021. Different uppercase letters indicate significant differences among the sampling times ($p < 0.05$). Dotted line represents mean flux for that sampling period. Dashed line marks 0. Shaded region represents nighttime sampling. Axes are not standardized to showcase individual patterns exhibited during each sampling day.*

3.2 Objective 2: Patch-specific physicochemical conditions

Water depth was greatest in the NoVeg patches and shallowest in the EmVeg patches throughout the summer (supplemental table S2) reaching its lowest point during campaign 2 (July) and peaking during campaign 3 (September) after heavy precipitation. Air and water temperature, relative humidity, PAR, and DO exhibited diel patterns. Relative humidity peaked at night (figure 6). Air and water temperature,

PAR and DO peaked during the day (figures 6, S4, S5). Water temperature was most variable at the surface with minimal diel change close to the sediment-water interface, resulting in large vertical temperature differences during the day. This dynamic was prominent in the SubVeg and NoVeg patches: on average, the max temperature difference between the top and the bottom of the water column in the SubVeg patch ranged from 4 – 9°C during the hottest time during the day and 4 – 8°C in the NoVeg patch (figure S6). Air pressure was variable throughout the study period but did not tend to undergo a diel pattern (figure 6).

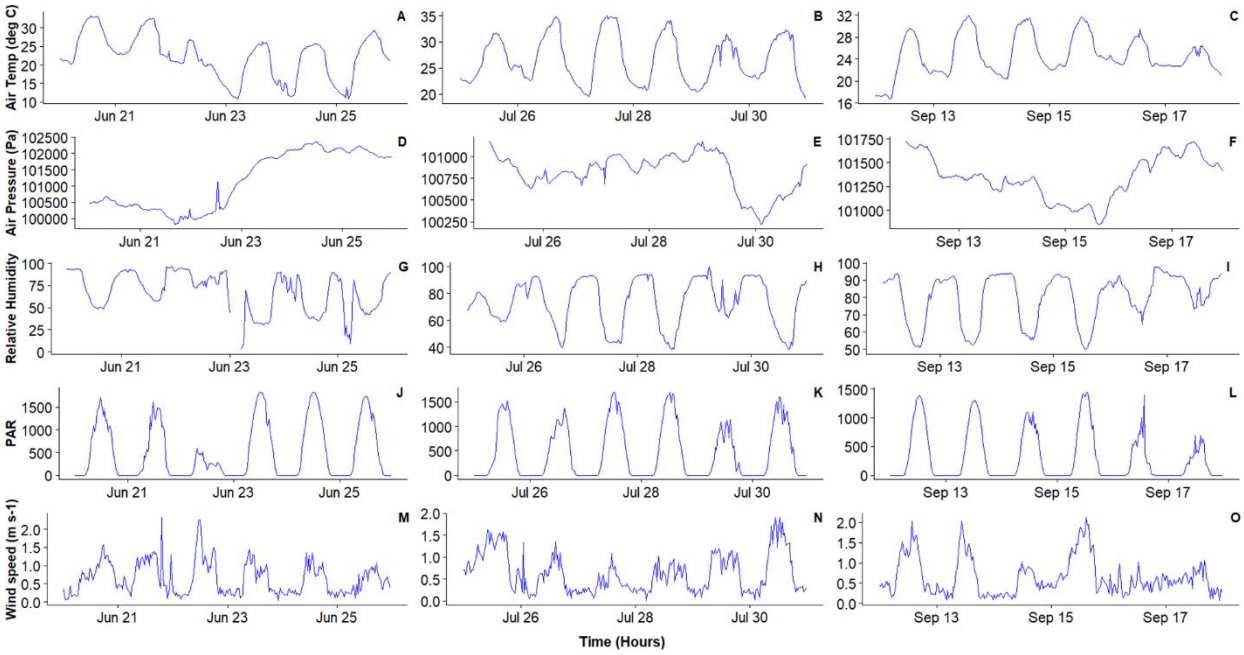

Figure 6*. Time series during each sampling campaign in the restored wetland showing diurnal changes in (A-C) air temperature (°C), (D-F) air pressure (Pa), (G-I) relative humidity (%), (J-L) PAR, (M-O) wind speed (m* s^{-1}*). All variables listed were measured by an eddy covariance flux tower on site.*

3.3 Objective 3: Relationship between CH_4 flux and physicochemical variables

Results of the correlation analyses are reported in the supplemental (table S3). The "general patterns" exploratory model explained some variability in CH_4 fluxes (R^2 = 0.47) and identified vegetation patch type and water table as dominant contributors to the model (%R^2 = 43.7% and 42.4% respectively) (table S4). Air pressure was also included in the model (%R^2 = 13%).

Results from the "patch specific diel patterns" exploratory modeling series varied by patch type. The emergent vegetation patch model explained some variability in the CH_4 flux data (R^2 = 0.24) and included water temperature, air temperature, RH, and PAR as metrics (table 1). Air temperature and PAR were the dominant contributors to the model (%R^2 = 44% and 27% respectively). Both metrics were negatively correlated with flux (r^2 = -0.28, $p < 0.001$ and -0.37, $p < 0.001$ respectively). Water temperature was positively correlated with flux (%R^2 = 16%, r^2 = 0.47, $p < 0.01$). The submerged aquatic vegetation patch model explained a similar amount of variability in the CH_4 flux data (R^2 = 0.29) and included water temperature and PAR as metrics (table 1). Water temperature contributed the most to the model (%R^2 =87%) and was significantly positively correlated with CH_4 flux (r^2 = 0.25, $p < 0.001$). The no vegetation patch model explained less variability in CH_4 flux data and included only and included only water temperature at the sediment-water interface as a metric (table 1). Water temperature was significantly positively correlated with flux (r^2 = 0.348, $p < 0.05$).

Table 1. *Summary of 3 multiple linear models of CH_4 flux using physicochemical variables that vary diurnally. Dominant contributor metrics are shown along with associated model parameters.*

Model	Metric	r	VIF	β	p value	Partial R^2	%R^2
	Water temperature	0.474	2.00	-0.02 ± 0.008	0.0097	0.08	15.9
Emergent Vegetation	Air temperature	-0.283	1.74	0.031 ± 0.007	0.000006	0.22	44.7
	RH	-0.244	4.23	-0.007 ± 0.003	0.026	0.06	11.9
R^2 = 0.24 ΔAIC =	PAR	-0.373	3.75	-0.0003 ± 0.0001	0.0005	0.14	27.6
Submerged Vegetation	Water Temperature	0.252	1.009	0.13 ± 0.03	0.000007	0.25	87.7
R^2 = 0.29 ΔAIC =	PAR	-0.035	1.099	0.0003 ± 0.0001	0.113	0.04	12.3
No Vegetation R^2 = 0.12 ΔAIC =	Water temperature	0.348	NA	0.07 ± 0.027	0.012	0.12	1

4. Discussion

Wetland methane emissions are known to be highly variable across space and time (Herbst *et al.* 2011) and this study shows that small-scale (< 1 m) patches dominated by different types of vegetation play an important role. Differences in the magnitude and temporal patterns in CH_4 flux were found for wetland patches dominated by emergent sedges (*Carex*), submerged aquatic vegetation (*Juncus*), and open water areas with no vegetation. Fluxes coming from the emergent or submerged patches were highest while the no vegetation patches were sometimes sinks for methane. Fluxes from emergent vegetation patches, while variable over time, did not display a consistent diel pattern which contradicts multiple studies (Duan *et al.* 2005; Chen *et al.* 2010). This contrasts with the other two patch types: fluxes consistently peaked at 1pm in the submerged vegetation patch and at 5am in the no vegetation patch.

As I discuss more fully below, the observed differences between flux patterns may be the result of different dominant transport mechanisms (i.e., plant-mediated transport in the vegetated patches vs. hydrodynamic transport in the non-vegetated patch), differences in plant productivity, or patch-related differences that co-vary with plant type (e.g., water depth was consistently lower in emergent vegetation patches). Regardless of underlying mechanisms this study points to two key results. First, small-scale chamber measurements of methane fluxes in patchy wetlands may not be representative of emissions even a few meters away. Second, diel variation in emissions can be great enough that one cannot assume a single measurement is representative of 24-hour flux.

4.1 Diurnal patterns of CH_4 fluxes in different vegetation patches

Spatially, Matthes *et al.* (2014) demonstrated using three eddy covariance flux towers distributed across a large flooded peatland that the spatial heterogeneity in wetlandscan lead to large variations in CH_4 flux across a single system (Matthes *et al.* 2014). Others have demonstrated that different types of vegetation cover (or lack thereof) can lead to wide ranges in CH_4 flux (Sun *et al.* 2013; Jeffrey *et al.* 2019). Commonly observed patterns indicate that emergent vegetation species tend to have higher fluxes compared to submerged aquatic species, and patches with vegetative cover tend to have higher fluxes than those without vegetation (Duan *et al.* 2005; Kao-Kniffin *et al.* 2010; Bhullar *et al.* 2013; Zhang *et al.* 2019). But these differences have not been as well explored on the diel scale. Temporally, Bansal *et al.* (2018) did show differences in fluxes from clipped vegetation patches sampled repeatedly over day/night using chamber methods, but their study did not fully address the role different vegetation cover types may have in influencing CH_4 flux patterns (Bansal *et al.* 2018). To the best of my knowledge, this is the first study to compare diel variability of CH_4 flux across emergent vegetation, submerged aquatic vegetation, and no vegetation patches simultaneously.

4.1.1 Emergent vegetation patches

The emergent vegetation patch did not display the degree of diel variability expected. Multiple studies have shown that patches dominated by emergent vegetation tend to display diel patterns in CH_4 fluxes, with higher fluxes occurring during the daytime (Duan *et al.* 2005; Chen *et al.* 2010; van den Berg *et al.* 2016). This is often attributed to variations in plant activity associated with changing light levels (Whiting

and Chanton 1996; Van der Nat *et al.* 1997) and may be associated with opening/closing of their stomata although direct measurements of stoma activity are rare (Yavitt and Knapp 1995). Morrisey *et al.* (1993) did find that stomatal conductance in *Carex* species may exert some control of CH_4 flux from plants, but they also suggest that cuticular conductance may play a role in facilitating flux. In the present study, diel patterns varied by sampling time and Carex was a constant source of CH_4 to the atmosphere at all times, which was also the case in the Morrisey *et al.* (1993) study. Certainly, the flux patterns found in this study and others may be associated with processes other than transport, including temporal and spatial variation in biogeochemical processes. Noyce and Megonigal (2021) proposed that some wetland plant species can be categorized as net rhizosphere oxidizers or net reducers which can influence methane production and consumption (Noyce and Megonigal 2021).

4.1.2 Submerged vegetation patches

Unlike the emergent vegetation patch, we found a repeated peak in CH_4 flux in the submerged vegetation patch. There are few studies that have focused on diel CH_4 fluxes from submerged aquatic species; however, Zhang *et al.* (2018) showed that for such plants (i.e., *Hydrilla verticillata* and *Potamogeton malaianus*) the fluxes tended to be much higher at night rather than the day (Zhang *et al.* 2018). They hypothesized it was likely due to lower plant activity levels reducing water column and soil oxygen levels and thus the potential for CH_4 oxidation (Sorell *et al.* 2002; Zhang *et al.* 2018). This was supported by two studies showing that submerged aquatic species can be associated with epiphytic methanotrophs that greatly reduce daytime CH_4 fluxes (Heilman *et al.* 2001; Yoshida *et al.* 2014). I observed the exact opposite: CH_4 fluxes

tended to be higher during the daytime and consistently peaked at 1pm, a pattern that mirrored peaks in PAR, DO, and temperature. While it is possible that the submerged vegetation is capable of transporting CH_4, the methane would be released into the water and still have to diffuse through the surface layer and into the atmosphere.

In the present study, the largest fluxes from submerged vegetation were at midday and the associated warmer temperatures may have increased the diffusion rate of CH_4 through the air-water interface. Work by Moradi *et al.* (2020) has demonstrated that increasing water temperature can increase the rate of CH_4 diffusion through the water column (Moradi *et al.* 2020). But increasing temperature is also known to promote increased production of methane and the lower water tables that were present in July at my site could have reduced the potential for CH_4 oxidation as gas moved toward the surface. While not included in the model, water depth was negatively correlated with CH_4 flux (table 1). The lower water depth in July could provide less of barrier for diffusive CH_4 flux from the vegetation through the water column, or it could mean previously submerged vegetation is partially emergent and can provide a direct conduit to the atmosphere. Again, there has been little work done on how *Juncus repens* impacts CH_4 cycling in wetland systems. More exploratory analyses will be needed to unravel how this species impacts the below-ground production, oxidation, and transport of CH_4.

4.1.3 No vegetation patches

Multiple studies suggest that CH_4 fluxes form unvegetated, open water patches tend to display some degree of diurnal variability, usually with higher nighttime fluxes (Godwin *et al.* 2013; Poindexter *et al.* 2016). This is thought to be due to thermal

stratification in the water column during the day leading to an accumulation of CH_4 in the lower layers of the water column (Van der Molen and Wijmstra 1994; Godwin *et al.* 2013). Eddies produced by nighttime cooling leading to turnover can potentially drive larger pulses of CH_4 flux (Godwin et al. 2013; Poindexter et al. 2016; Sieczko et al. 2020). While the fluxes I observed from the no vegetation patches were low throughout the summer, they did consistently peak at night. I also consistently saw peaks at 5am, that coincided with the time when the water column was potentially mixed. The water column was stratified during the day and mixed at night due to convection (figure S3) which supports the hypothesis that the higher nighttime fluxes may be due to the breakdown of stratification and mixing in the water column. Confirming this requires a study that better pairs flux measurements with the timing of this potential breakdown.

4.2 Potential drivers of CH_4 fluxes

Across all patch types, temperature was a dominant contributor to explaining variability in CH_4 flux which is consistent with multiple studies showing it to be a dominant driver of CH_4 production and emissions (Tian *et al.* 2011; Masamba *et al.* 2015; Yang *et al.* 2017). Perez *et al.* (2015) and Bansal *et al.* (2016) have argued that when the water table is above a critical depth, temperature is the primary driver of variability in CH_4 flux. This study supports that argument: water depth did not change significantly on a diel scale, and both air and water temperature varied greatly. Water temperature in all three patches may have played a role in increasing CH_4 production, with warmer temperatures promoting increased rates of methanogenesis. In the submerged and no vegetation patches, temperature also may have played a role in

promoting CH_4 transport. The thermal stratification and mixing in the no vegetation patch may have contributed to larger fluxes at night. In the submerged vegetation patch, warmer temperatures in the water column during midday might have increased the rate of production or diffusion of CH_4 being transported to the water column via the vegetation.

The emergent vegetation model highlighted an interesting relationship between CH_4 flux and air temperature, PAR, and relative humidity: the CH_4 flux was negatively correlated with all three metrics. The relationship with air temperature seems counterintuitive: since warmer temperatures are typically associated with increased CH_4 production and subsequent flux. This dynamic could possibly be related to O_2 transport. It may be that *Carex* creates a net oxidizing environment in its rhizosphere, so during times when there's increased plant activity (i.e., when PAR is higher), there is less flux. This patch also showed a positive correlation between CH_4 flux and water temperature; this relationship may be production related such that warmer temperatures promoted increased rates of methanogenesis.

While it did not vary over the diel scale, the changes in water table depth within each patch helped explain some variability that existed between campaigns, specifically in the no vegetation patch. This was most likely because the depth of the water directly affected the distance CH_4 would have to travel from the sediment to the surface. Without vegetation to mediate CH_4 transport, the main transport mechanisms are diffusion/hydrodynamic transport and ebullition. Diffusion alone is slow and leaves CH_4 susceptible to potential oxidation for longer periods (Milberg et al. 2017). The large increase in CH_4 fluxes observed in July (when the water table was at its lowest

point) suggests that water table depth acted as a barrier to CH_4 transport in this patch. Separating the effect of water table depth from other factors that influence fluxes would require measurements over a wider range of water table depths.

5. Conclusions and implications for future studies

I show that diel patterns in wetland systems are strongly linked to the dominant vegetation cover of a patch. Whether the differences in patterns among patch types are a result of vegetation impact on the production, oxidation, and/or transport of CH_4 and/or patch-specific conditions that co-vary with plant type will require extended study. Regardless, to improve estimates of CH_4 fluxes, future models need to account for the spatial distribution of patches within a wetland system, and how patch fluxes may vary on a diel scale. Many chamber-based studies operate on the assumption that one measurement taken during midday will be a representative estimate of CH4 fluxes for an entire 24-hour period (Pennock et al. 2010; Bansal et al. 2018). This work demonstrates that that may not be an appropriate method for all vegetation patch types across all systems: a midday sample was representative of the 24-hour average flux in the patch dominated by emergent vegetation; the same was not true for the patches with submerged and no vegetation. While this study contributes to the growing understanding of how CH_4 patterns vary spatially over diel cycles, more studies are needed across a range of vegetation types and wetland systems as the results may be system specific. More work like this will help improve CH_4 estimates at the local, regional, and global level.

Supplemental

Table S1. *Maximum, minimum and mean of CH4 emissions (mg CH4 -C-m-2h-1) for emergent vegetation (EmVeg), submerged aquatic vegetation (SubVeg), and no vegetation (NoVeg) patches throughout the study period in 2021 (n = 5). Different lowercase letters indicate significant differences between daily mean flux (significance $p < 0.05$).*

CH_4 emissions ($mg\ CH_4\text{-}C\text{-}m^{-2}h^{-1}$)		**Measurement occasion**				
		June 20th-21st	**June 23rd-24th**	**July 26th-27th**	**July 28th-29th**	**Sept 12th-13th**
EmVeg	Maximum	22.8 – 30.0	25.67	24.99	23.21	46.76
	Minimum	13.14	6.77	14.62	10.74	9.43
	Mean	**21.87^{a}**	**13.36^{b}**	**20.20^{a}**	**16.82^{ab}**	**20.12^{a}**
SubVeg	Maximum	94.69	46.72	153.30	350.75	28.08
	Minimum	4.51	-0.27	2.12	2.18	-1.19
	Mean	**23.79^{a}**	**6.23^{a}**	**31.11^{a}**	**90.62^{b}**	**5.07^{a}**
NoVeg	Maximum	3.28	0.81	20.37	10.87	1.31
	Minimum	-4.88	-0.55	-0.68	0.10	-1.70
	Mean	**0.37^{a}**	**0.26^{a}**	**4.02^{b}**	**3.52^{b}**	**0.05^{a}**

CO_2 Results

Below are CO_2 flux measurements from EmVeg (Figure S5), SubVeg (Figure S6), and NoVeg (Figure S7). Villa *et al.* suggested that CH_4 fluxes and CO_2 fluxes would be positively correlated if CH_4 flux is dependent on stomatal conductance (Villa *et al.* 2020). There were no significant correlations in any patch type.

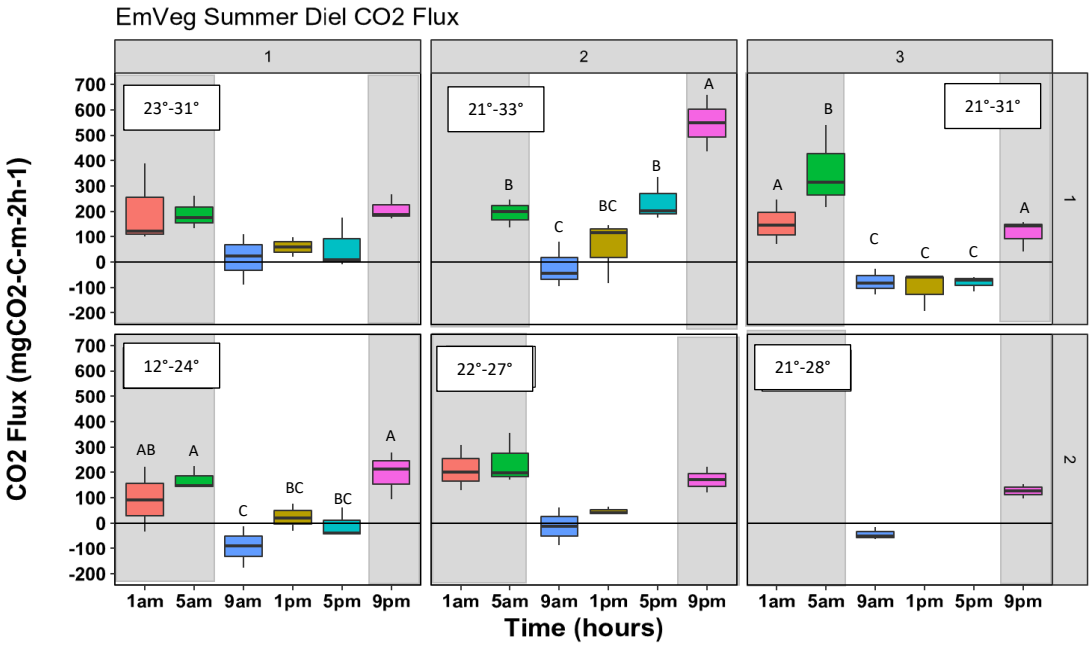

Figure S1. *EmVeg diel CO_2 Flux. Columns (1-3) represent sampling campaign. Rows (1-2) represent day of sampling during each campaign. Different uppercase letters indicate significant differences among the sampling times. Text box inserts show the temperature range (deg C) during the time of sampling*

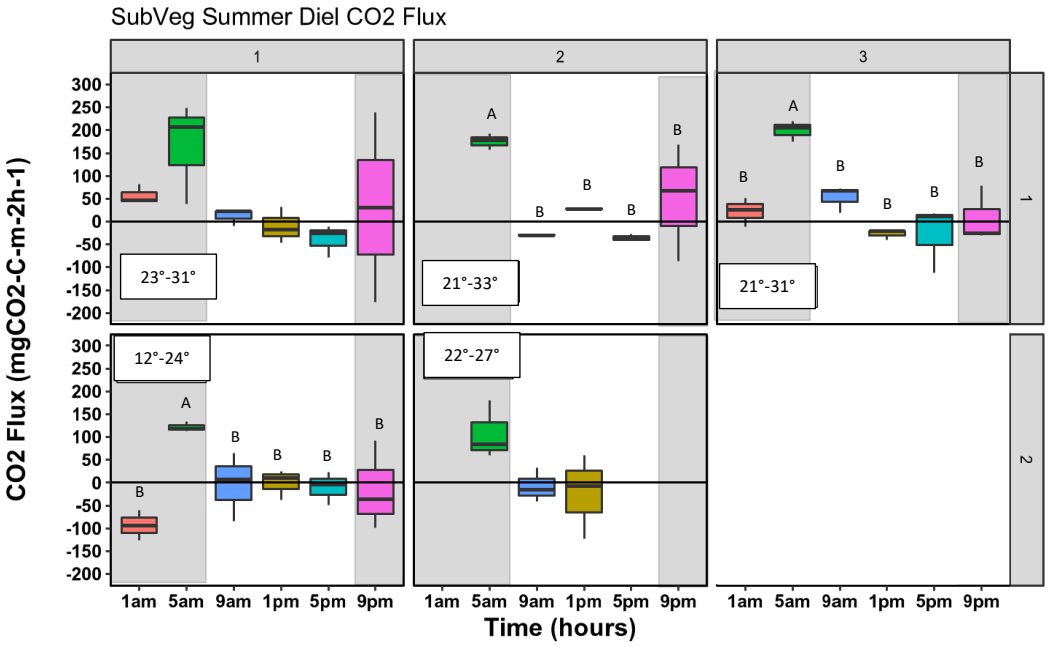

Figure S2. *SubVeg diel CO_2 flux. Columns (1-3) represent sampling campaign. Rows (1-2) represent day of sampling during each campaign. Different uppercase letters indicate significant differences among the sampling times. Text box inserts show the temperature range (deg C) during the time of sampling.*

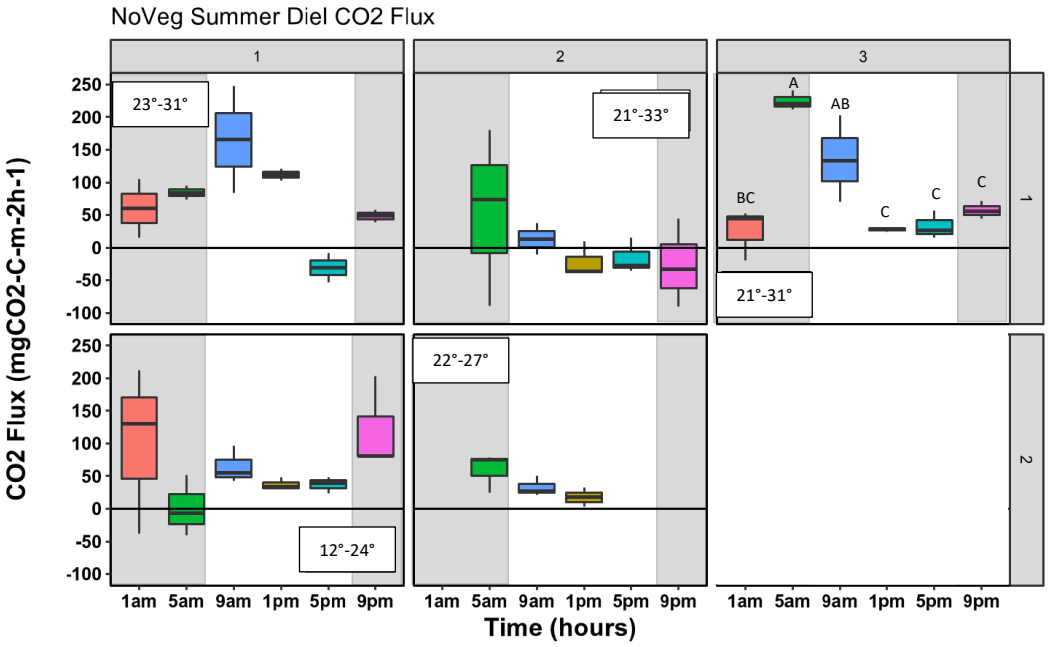

Figure S3*. NoVeg diel CO_2 Flux. Columns (1-3) represent sampling campaign. Rows (1-2) represent day of sampling during each campaign. Different uppercase letters indicate significant differences among the sampling times. Text box inserts show the temperature range (deg C) during the time of sampling*

Table S2. *Water depth (m) in each patch during the campaigns.*

	Campaign		
Patch	June 20th-24th	July 26th-29th	Sept 12th-15th
EmVeg	0.25	0.13	0.33
SubVeg	0.44	0.36	0.58
NoVeg	0.59	0.43	0.69

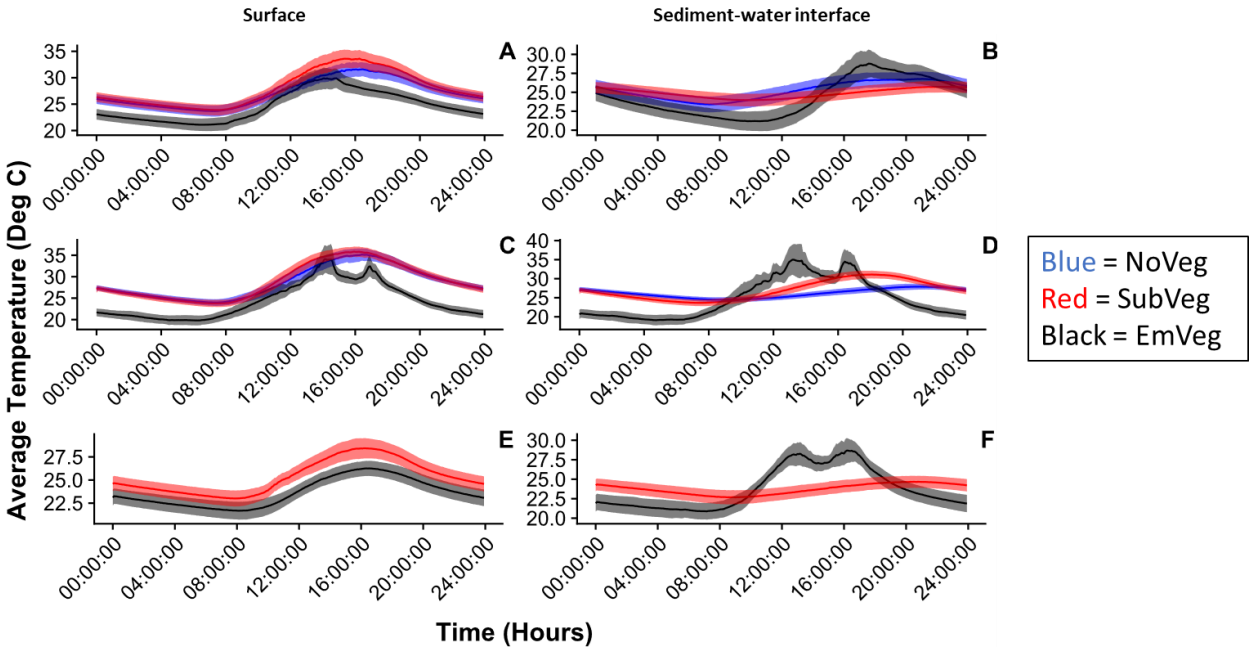

Figure S4*. Average temperature (°C) in the Top (left) and Bottom (right) of the water column. Red line is SubVeg patch, blue is the NoVeg patch, and black is the EmVeg patch. Line's represent the mean, and shaded areas represent confidence interval. Figures A-B are June 20th – 27th, C-D are July 20th – 28th, and E-F are September 13th – 20th.*

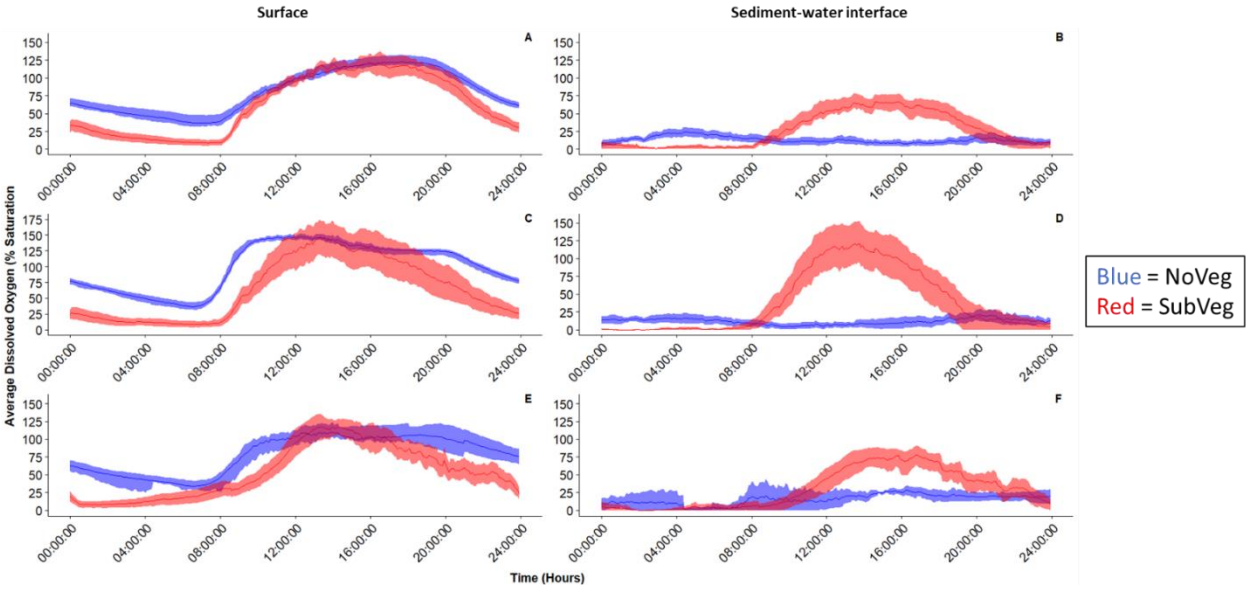

Figure S5*. Average dissolved oxygen (% saturation) in the Top (left) and Bottom (right) of the water column. Red line is SubVeg patch and the blue is the NoVeg patch. Lines represent the mean, and shaded areas represent confidence interval. Figures A-B are June 20th – 27th, C-D are July 20th – 28th, and E-F are September 13th – 20th.*

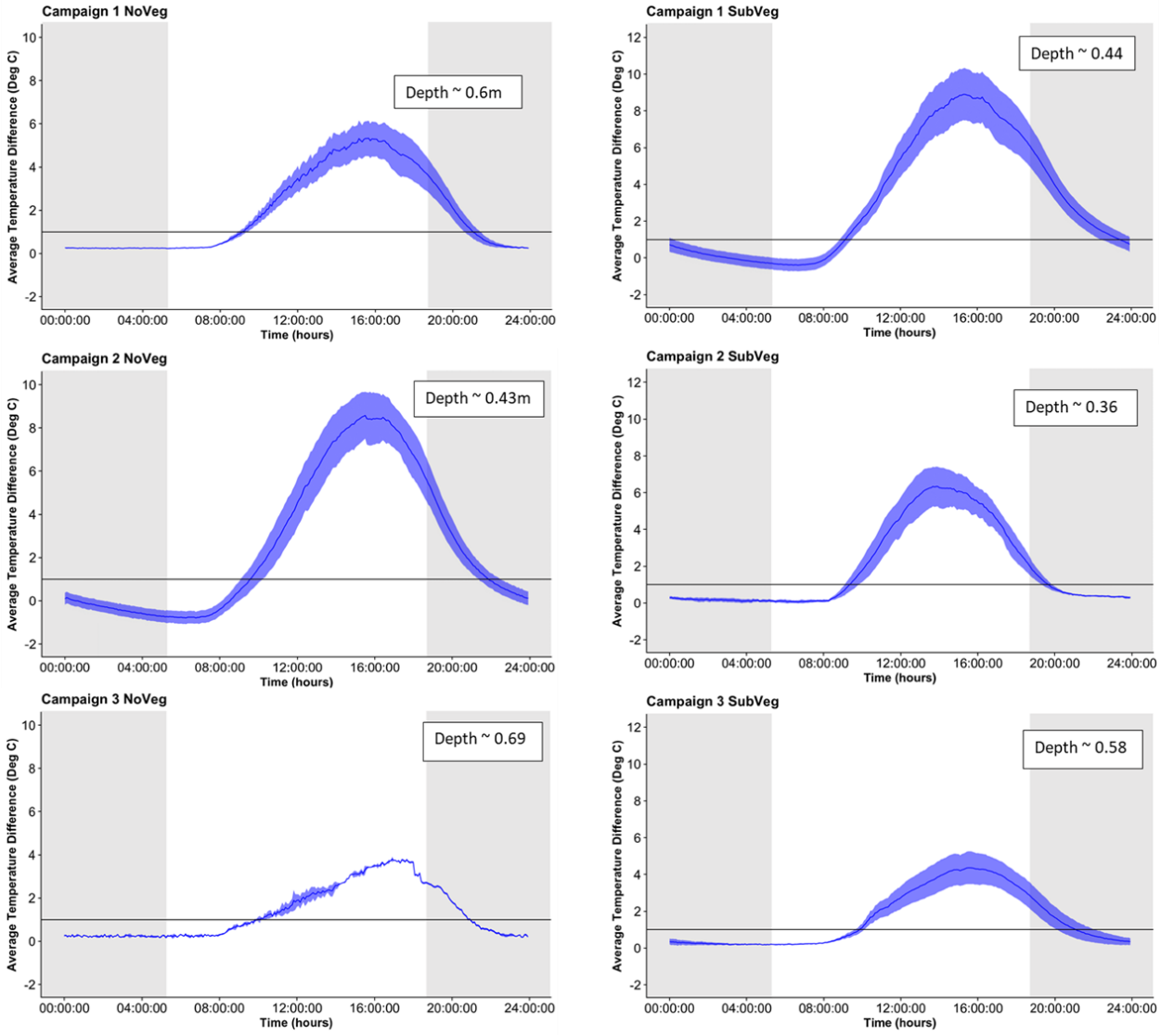

Figure S6*. Average temperature difference (°C) between the top and the bottom of the water column in the NoVeg patch (left) and SubVeg patch (right) across all three campaigns. Insets are approximate water column height (m). Horizontal line is at 1°C. Line's are mean's and shaded space are the confidence interval. Shaded bars on the figure represent approximate nighttime hours*

Table S3. *Kendall's correlation coefficients between abiotic variables and methane (CH_4) flux rates for each patch type: Emergent vegetation, submerged aquatic vegetation, and no vegetation, for N = 89 – 108 samples.*

Covariate	**Correlation coefficient (τ)**		
	Emergent Vegetation	**Submerged Vegetation**	**No Vegetation**
Water pH at the sediment-water interface	0.04	-0.19	-0.17
Water pH just below the surface	0.091	**-0.16***	-0.023
Water temperature ~1 cm below the surface	**0.22****	**0.31*****	0.12
Temperature mid-water column	**0.17***	**0.36*****	**0.2***
Water temperature at the sediment-water interface	0.0054	**0.39*****	**0.35*****
Temperature difference between the surface and sed/water interface	-	-0.13	0.13
Water depth	-0.041	**-0.43*****	**-0.25***
Air temperature	**0.18***	**0.25****	0.079
Air pressure	**-0.25*****	**-0.35*****	**-0.32*****
Relative humidity	-0.052	-0.046	**0.2***
Wind speed	0.1	**0.2***	0.015
PAR	0.037	0.11	0
Dissolved oxygen concentration at the sediment-water interface	-	0.022	-0.071
Dissolved oxygen concentration just below the water surface	-	0.21	-0.46
Biomass	**-0.15***	-	-

Table S4. *Summary of multiple linear model of CH_4 flux using all physicochemical variables and patch type. Dominant contributor metrics are shown along with associated model parameters.*

Metric	r	VIF	β	p value	Partial R^2	%R^2
Patch	-0.309	3.1	-0.421 ± 0.09	0.000002	0.095	43.7
Air pressure	-0.303	1.1	-1.17 ± 0.09	0.00908	0.03	13.8
Water depth	-0.173	3.2	-0.0003 ± 0.00006	0.000003	0.092	42.4

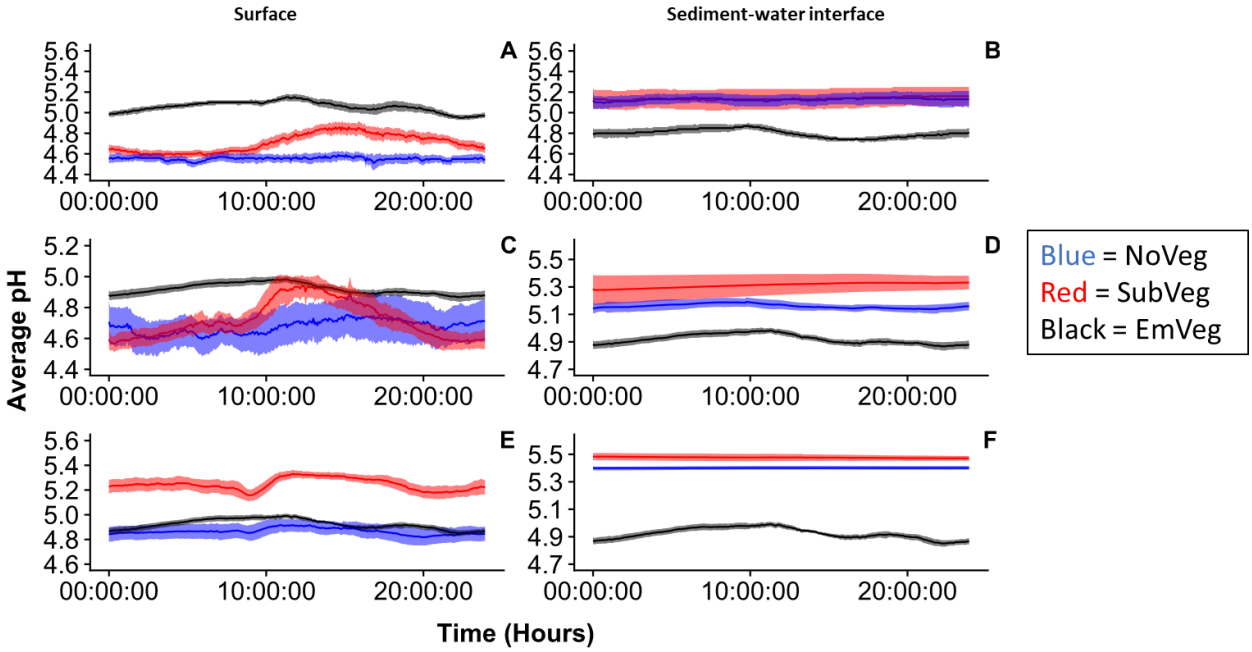

Figure S7*. Average pH in the Top (left) and Bottom (right) of the water column. Red line is SubVeg patch, blue is the NoVeg patch, and black is the EmVeg patch,. Line's represent the mean, and shaded areas represent confidence interval. Figures A-B are June 20th – 27th, C-D are July 20th – 28th, and E-F are September 13th – 20th.*

Supplemental Methods

Table S1. *Parts used to make to make the floating chambers used in the Sub and NoVeg patches described here. Building material quantity is specified for one chamber only.*

Type	Part	Dimensions	Brand	Quantity
Chamber	Arylic Aquarium	40 cm x 40 cm x 40 cm	Glass cages	1
Float	PVC pipe	Nominal Inside Pipe Diameter (In.): 2" ~ 46 cm long	Home depot	4
	PVC caps	Camps for 2" diameter pipes	Home depot	8
	8 oz. Purple CPVC and PVC Primer and Regular Clear PVC Cement Combo Pack	-	Oatey	-
	SwimWays Super Swim Noodle	-	Dick's sporting goods	~3
Sampling port	Tygon tubing	3/8 in. I.D. x 1/2 in. O.D.	UDP	-
	Stop cock	-	Zocakee	1
Handles	3/4 in. x 1 ft. Polypropylene Twist Rope, Yellow	-	Everbilt	-
Miscelaneous	11 in. UV Cable Tie, Black (Zip ties)	-	Commercial Electric	-
	ductape	-	-	-
	Clear Silicone 2.7 fl. oz. Waterproof Sealant	-	Locite	-

Building Instructions

1. Cut PVC pipes so that they are approximately 46 cm long.
2. Seal cap on one side of pipe using primer and PVC cement.
3. Fill PVC pipe with pool noodle to capacity.
4. Seal cap on other side using primer and PVC cement.
5. Drill hole large enough to fit tygon tubing through in the center of the chamber top.
6. Drill 1 holes approximately 3 cm up from the bottom of the aquarium and 4 cm in from the left side on each side.
7. Repeat step 6 drilling a hole on the right side of on every side of the aquarium.
8. Use zip ties to attach PVC floats on each side of the aquarium. If needed, for additional support/buoyancy, add additional swim noodles cut down to size onto the floats as needed. I used approximately 4 zip ties per float.

9. Insert tygon tubing (cut down to approximately 5 cm (or enough that there is tygon tubing extending into the chamber and out into the open air).
10. Use sealant/ductape to attach stopcock to the tygon tubing.
11. Use sealant and ductape to create a secure seal between the tygon tubing and the chamber.

Bibliography

Baldoicchi, D. D. *et al.* (2012). The challenges of measuring methane fluxes and concentrations over a peatland pasture. *Agriculture for Meteorol.* 153: 177-187.

Bansal, S. et al. (2016). Temperature and Hydrology Affect methane emissions from prairie pothole wetlands. *Wetlands*. 36: 371-381.

Bansal, S. et al. (2018). Diurnal Patterns of Methane Flux from a Seasonal Wetland: Mechanisms and Methodology. *Wetlands* 38: 993-943.

Bansal, S. et al. (2020). Vegetation Affects Timing and Location of Wetland Methane Emissions. *Journal of Geophysical Research: Biogeosciences* 125, e2020JG005777. DOI: 10.1029/2020JG005777.

Bastviken, D. *et al.* (2020). Technical note: Facilitating the use of low-cost methane (CH_4) sensors in flux chambers – calibration, data processing, and an open-source make-it-yourself logger. *Biogeosciences* 17(13): 3659-3667.

Bhullar, G. S. et al. (2013). Variation in the plant-mediated methane transport and its importance for methane emission from intact wetland peat mesocosm. *Journal of Plant Ecology* 6(4): 298-304.

Bridgham, S. D. et al. (2013). Methane emissions from wetlands: biogeochemical, microbial, and modeling perspectives from local to global scales. *Global Change Biology* 19: 1325-1346.

Chen, H. *et al.* (2008). Determinants influencing seasonal variations of methane emissions from alpine wetlands in Zoige Plateau and their implications. *Journal of Geophysical Research* 113: D12303, doi:10.1029/2006JD008072.

Chen, H. *et al.* (2010). Diurnal variation of methane emissions from an alpine wetland on the eastern edge of Qinghai-Tibetan Plateau. *Environ Monit Assess* 164: 21-28.

Duan, X. *et al.* (2005). Seasonal and diurnal variations in methane emissions from Wuliangsu Lake in arid regions of China. *Atmospheric Environment* 39: 4479-4487.

Fenstermacher, D. E. *et al.* (2014). Distribution, Morphometry, and Land Use of Delmarva Bays. 34: 1219-1228.

Fisher, T. R. *et al.* (2006). History of land cover change and biogeochemical impacts in the Choptank River basin in the mid-Atlantic region of the US. *International Journal of Remote Sensing* 27(17): 3683-3703.

Godwin, C. M. *et al.* (2013). Evening methane emission pulses from a boreal wetland correspond to convective mixing in hollows. *Journal of Geophysical Research: Biogeosciences* 118: 994-1005.

Heilman, M. and Carlton, R. (2001). Methane oxidation associated with submersed vascular macrophytes and its impact on plant diffusive methane flux. *Biogeochemistry.* 52(2): 207-224.

Henneberger, R. *et al.* (2016). Diurnal Patterns of Greenhouse Gas Fluxes in a Swiss Alpine Fen. *Wetlands* 37: 193-204.

Herbst, M. T. *et al.* (2011). Interpreting the variations in atmospheric methane fluxes observed above a restored wetland. *Agric. For. Meterol.* 151(7): 841-853.

Jeffrey, L. C. *et al.* (2019). Wetland methane emissions dominated by plant-mediated fluxes: Contrasting emissions pathways and season within a shallow

freshwater subtropical wetland. *Limnology and Oceanography* 64: 1895-1912.

Kao-Kniffin, J. *et al.* (2010). Methane dynamics across wetland species. *Aquatic Botany*. 93(2): 107-113.

Knoblauch, C. *e al.* (2015). Regulation of methane production, oxidation, and emission by vascular plants and bryophytes in ponds of the northeast Siberian polygonal tundra. *Journal of Geophysical Research: Biogeosciences*. 120(12): 2525-2541.

Lovelock, C. (2014). How to Estimate Carbon Dioxide Emissions. Coastal Blue Carbon: Methods for Assessing Carbon Stocks and Emissions Factors in Mangroves, Tidal Salt Marshes, and Seagrasses. Edited by J Howard et al. Arlington, VA: Conservation International, Intergovernmental Oceanographic Commission of UNESCO, International Union for Conservation of Nature, p. 109–122.

Matthes, J. *et al.* (2014). Parsing the variability in CH4 flux at a spatially heterogeneous wetland: Integrating multiple covariance towers with high-resolution flux footprint analysis. *Journal of Geophysical Research: Biogeosciences*. 119: 1322–1339.

McDonough, O. T. *et al.* (2015). Surface Hydrologic Connectivity Between Delmarva Bay Wetlands and Nearby Streams Along a Gradient of Agricultural Alteration. *Wetlands* 35:41-53.

Masamba, W. *et al.* (2015). Physiochemical controls of diffusive methane fluxes in the Okavango Delta, Botswana. *Wetlands Ecology and Management.* 23(4): 617-635.

Mikkela, C. (1995). Diurnal variation in methane emission in relation to the water table, soil temperature, climate and vegetation cover in a Swedish acid mire. *Biogeochemistry* 28: 93-114.

Milberg, P. *et al.* (2017). Temporal variations in methane emissions from emergent aquatic macrophytes in two boreonemoral lakes. *AoB Plants* 9: plx029; doi:10.1093/aobpla/plx029.

Moradi, H. *et al.* (2020). Prediction of methane diffusion coefficient in water using molecular dynamics simulation. *Heliyon*. 6(11): e05385.

Morin, T. H. *et al.* (2014). The seasonal and diurnal dynamics of methane flux at a created urban wetland. *Ecological Engineering* 72: 74-83.

Morrisey, L. A. *et al.* (1993). Significance of stomatal control on methane release from Carex-dominated wetlands. *Chemosphere*. 26(1-4): 339-355.

Neubauer, S. C. and Megonigal, J. P. (2015). Moving Beyond Global Warming Potentials to Quantify the Climatic Role of Ecosystems. *Ecosystems* 18: 1000-1013.

Neubauer, S.C. and Megonigal, J. P. (2022). Biogeochemistry of Wetland Carbon Preservation and Flux. Chapter 3 In: Wetland Carbon and Environmental Management, Geophysical Monograph 267, Edited by Ken W. Krauss, Zhiliang Zhu, and Camille L. Stagg. *American Geophysical Union*. DOI: 10.1002/9781119639305.ch3

Pennock, D. *et al.* (2010). Landscape controls on N2O and CH4 emissions from freshwater mineral soil wetlands of the Canadian prairie pothole region. *Geoderma* 155:308–319.

Pérez, C. *et al.* (2015). Overriding control of methane flux temporal variability by water table dynamics in a southern Hemisphere, raised bog. *Journal of Geophysical Research: Biogeosciences*. 120: 673-692.

Phillips, P. J. and Shedlock R. J. (1993). Hydrology and chemistry of groundwater and seasonal ponds in the Atlantic coastal plain in Delaware, USA. *Journal of Hydrology* 141:151-178.

Poindexter, C. M. *et al.* (2016). The contribution of an overlooked transport process to a wetland's methane emissions. *Geophysical Research Letters* 43: 6276-6284.

R Core Team(2022). R: A Language and environment for statistical computing. R foundation for Satistical Computing, Vienna Austria. URL: https://www.R-project.org/.

Rochette, P. and Eriksen-Hamel, N. S. (2008). Chamber Measurements of Soil Nitrous Oxide Flux: Are Absolute Values Reliable? *Soil Sci. Soc. Am. J.* 72: 331-342.

Sieczko, A. K. *et al.* (2020). Diel variability of methane emissions from lakes. *PNAS* DOI: 10.1073/pnas.2006024117.

Sorrell, B.K. *et al.* (2002). Methanotrophic bacteria and their activity on submerged aquatic macrophytes. Aquat. Bot. 72, 107–119.

Ström, L. *et al.* (2005). Species-specific Effects of Vascular Plants on Carbon Turnover and Methane Emissions from Wetlands. *Biogeochemistry* 75:65-82.

Sun, L. *et al.* (2013). Temporal and spatial variability of methane emissions in a northern temperate marsh. *Atmospheric Environment* 81: 356-363.

Tian, J. *et al.* (2011). Methane production in relation with temperature, substrate and soil depth in Zoige wetlands on Tibetan Plateau. *Acta Ecologica Sinica*. 31: 121-125.

Temmink, R. J. *et al.* (2022). Recovering wetland biogeomorphic feedbacks to restore the world's biotic carbon hotspots. *Science.* 376. eabn1479.

van den Berg, M. *et al.* (2016). The role of *Phragmites* in the CH_4 and CO_2 fluxes in minerotrophic peatland in southwest Germany. *Biogeosciences*. 13: 6107 – 6119.

Van der Molen, P. C. and Wijmstra, T. A. (1994). The thermal regime of hummock-hollow complexes on clara bog, CO Offaly. *Biology and Environment* 94B(3): 209-221.

Van der Nat, F. J. *et al.* (1997). Spatial distribution and inhibition by ammonium of methane oxidation in intertidal freshwater marshes. *Appl. Environ. Microbiol.* 63: 4,734–4,740

Villa, J. *et al.* (2020). Plant-mediated methane transport in emergent and floating-leaved species of a temperate freshwater mineral-soil wetland. *Limnology and Oceanography*. 65(7): 1635-1650.

Villa, J. A. *et al.* (2021). Ebullition dominates methane fluxes from the water surface across different ecohydrological patches in a temperate freshwater marsh at

the end of the growing season. *Science of the Total Environment*. 767: 144498.

Whiting, G. J. and Chanton, J. P. (1996) Control of the diurnal pattern of methane emissions from emergent aquatic macrophytes by gas transport mechanism. *Aquatic Botany* 54: 237-253.

Wilson, J. O. *et al.* (1989). Seasonal variation of methane emissions from a temperate swamp. *Biogeochemistry* 8: 55-71.

Woolway, R. I. *et al.* (2014). A novel method for estimating the onset of thermal stratification in lakes from surface water measurements. *Water Resources Research*. 50(6): 5131-5140.

Yang, W. et al. (2017). Diurnal variation of CO2, CH4, and N20 emission fluxes continuously monitored in-situ in three environmental habitats in a subtropical estuarine wetland. Marine Pollution Bulletin 119: 289-298. Tyler et al. 2015

Yavitt, J. B. and Knapp, A. K. (1995). Methane emission to the atmosphere through emergent cattail (*Typha latifolia* L.) plants. *Tellus B.* 47(5): 521-534.

Yepsen, M. *et al.* (2014). Agricultural wetland restorations on the USA Atlantic Coastal Plain achieve diverse native wetland plant communities but differ from natural wetlands. *Agriculture, Ecosystems and Environment* 197: 11-20.

Yoshida, N. *et al.* (2014). Aquatic plant surface as a niche for methanotrophs. *Frontiers in Microbiology*. 5: 1-9.

Yu, L. *et al.* (2013). A comparison of methane emission measurements using eddy covariance and manual and automated chamber-based techniques in Tibetan Plateau alpine wetland. *Environmental Pollution* 181: 81-90.

Zhang, M. *et al.* (2019). Methane flux dynamics in a submerged aquatic vegetation zone in a subtropical lake. *Science of the Total Environment.* 672: 400-409.